Mechanical properties of cross-linked polymer particles prepared by nitroxide-mediated radical polymerization in aqueous micro-suspension

Tanaka, Takuya
Suzuki, Toyoko
Saka, Yuichi
Zetterlund, Per B
Okubo, Masayoshi

(Citation)
Polymer,48(13):3836-3843

(Issue Date)
2007-06

(Resource Type)
journal article

(Version)
Accepted Manuscript

Mechanical Properties of Cross-linked Polymer Particles Prepared by Nitroxide-Mediated Radical Polymerization in Aqueous Micro-Suspension

Takuya Tanaka,[1] Toyoko Suzuki,[2] Yuichi Saka,[1] Per B. Zetterlund,[2] Masayoshi Okubo[1,2]*

[1] Graduate School of Science and Technology, Kobe University, Kobe 657-8501, Japan.
Fax: +81-(0)78-8036161; E-mail: okubo@kobe-u.ac.jp

[2] Department of Chemical Science and Engineering, Faculty of Engineering, Kobe University, Kobe 657-8501, Japan.

Part CCXCI of the series "Studies on Suspension and Emulsion"

Abstract

The compressive strengths of micron-sized, cross-linked poly(styrene-divinylbenzene) particles synthesized by conventional radical copolymerization (70°C) and nitroxide (TEMPO)-mediated radical copolymerization (125°C) in aqueous micro-suspension have been measured. In the conventional system, the breaking energies and the compressive strengths of the particles (after removal of unreacted monomer) remained approx. constant from low to high conversion, whereas in the NMP system, both quantities increased close to linearly with conversion. The results suggest that the network formation is more homogeneous in the NMP system than in the conventional system.

Keywords: Compressive strength; Deformation; Cross-linking; Controlled/living radical polymerization

1. Introduction

The synthesis of micron-sized, cross-linked polymer particles is an active area of research with numerous applications in the biomedical and microelectronics fields. Synthetic approaches to such particles include seeded emulsion polymerization in connection with the dynamic swelling method [1], and seeded (or different variants thereof) dispersion polymerization [2-4]. Recent years have seen further development of these methods for the preparation of micron-sized, cross-linked polymer particles with a hollow structure and polymeric capsules containing perfume, magnetite and paraffin [5-7]. The cross-linked network strongly influences the mechanical properties of such particles, as exemplified by our previous work on non-spherical polymer particles with "rugby ball-like" and "red blood corpuscle-like" shapes resulting from (reversible) partial collapse of hollow spherical particles. Such shape transformation is closely related to the mechanical strength of the shell, which in turn is dictated by the nature of the cross-linked network. Thus, a quantitative mechanistic understanding of network formation is crucial in order to optimize cross-linked polymer particle synthesis for a specific application.

Controlled/living radical polymerization (CLRP) has attracted much attention recently as it provides a free radical synthetic route to polymers with narrow molecular weight distribution (MWD) and predetermined molecular weight (MW), as well as various complex architectures [8]. To date, the very vast majority of research on CLRP deals with linear (non-cross-linking) systems. However, CLRP can also be employed in connection with cross-linking systems [9-18]. Ide and Fukuda [9,10] showed that nitroxide-mediated radical (co)polymerization (NMP [19,20]; one of the available CLRP techniques) of styrene (S) and 4,4'-divinylbiphenyl in bulk using the nitroxide

2,2,6,6-tetramethylpiperidinyl-1-oxy (TEMPO) proceeded with lower apparent pendant reactivity than the corresponding conventional system. The higher apparent pendant reactivity in the conventional system is a consequence of an enhanced local concentration of pendants around the radical chain end due to the much higher primary chain-length (the MWs in CLRP are generally much lower than in a conventional system), which thus results in high levels of intramolecular cross-linking at low polymer concentrations. This local concentration effect is much less pronounced in CLRP, resulting in more homogeneous network formation without microgels, higher swelling and anticipated superior mechanical properties [10]. These findings are not specific to NMP; similar results have been reported for atom transfer radical polymerization (ATRP) [11-14] and reversible addition-fragmentation chain transfer (RAFT) [21].

Industrial application of CLRP, as well as environmental considerations, have provided a driving force for recent efforts to implement CLRP in aqueous dispersed polymerization systems [22-28]. We have recently reported that the TEMPO-mediated radical copolymerization of S and divinylbenzene (DVB) in aqueous miniemulsion proceeds with much lower pendant reactivities (i.e. lower cross-link density) than in the corresponding bulk system [29,30]. Based on these findings, as well as the intrinsic differences between conventional (i.e. non-living) cross-linking systems and cross-linking CLRP as described above, it is expected that the mechanical properties of cross-linked polymer particles prepared by CLRP exhibit different mechanical properties than cross-linked particles prepared by conventional radical polymerization.

In the present study, the breaking energy, the compressive strength and the deformation at break of P(S/DVB) particles prepared by conventional radical copolymerization and TEMPO-mediated radical copolymerization were compared. Micron-sized S/DVB droplets were prepared by the Shirasu Porous Glass (SPG) membrane emulsification technique [31]. The results are discussed in terms of the differences in the development of the polymer network between the two systems.

2. Experimental section

2.1. Materials

S was purified by distillation under reduced pressure in a nitrogen atmosphere. DVB (32% *p*-DVB, 68% *m*-DVB; Nippon Steel Chemical; purity 99%) was washed with 1 N NaOH and distilled water to remove inhibitors. Benzoyl peroxide (BPO) was recrystallized using chloroform/methanol. TEMPO (Aldrich) was used as received. Poly(vinyl alcohol) (PVA; Gohsenol GH-17: degree of polymerization, 1700; degree of saponification, 88%) was supplied by

Nippon Synthetic Chemical (Osaka, Japan).

2.2. SPG emulsification and micro-suspension polymerization

Micro-suspension polymerizations (9.1 wt.-% solids content based on 100% conversion to polymer) were performed as follows: Organic phase (conventional radical polymerization): S (4.94 g; 99 mol-% rel. to monomer), DVB (62 mg; 1 mol-% rel. to monomer). Organic phase (NMP): Same as above, except that TEMPO (19 mg; 2.22×10^{-2} M), and BPO (17 mg; 1.29×10^{-2} M) were also added. Polymerizations were also carried out in the absence of DVB using the same recipes as above, but with 4.99 g S. Aqueous phase: PVA (0.5 g; 10 wt.-% rel. to monomer). Emulsification was carried out using Shirasu Porous Glass (SPG) technology (SPG Technology Co., Ltd., Japan) employing a microporous glass membrane with pore size 1.3 μm. The resulting emulsions were transferred to glass ampoules (each ampoule contained approximately10 mL), degassed using several N_2/vacuum cycles and sealed off under vacuum. The polymerizations were carried out at 70°C (conventional radical polymerization) and 125°C (NMP) shaking the ampoules horizontally at a rate of 100 cycles/min. The polymer particles obtained were observed with an optical microscope (ECLIPSE 80i, Nikon Corporaiton, Tokyo, Japan).

The polymer particles prepared by conventional radical polymerization for mechanical testing were isolated from the aqueous dispersions by evaporation of water and unreacted monomer under vacuum at room temperature (not to complete dryness, but until a very concentrated emulsion was obtained). An aqueous solution of PVA (the water added contained PVA to avoid coagulation, which otherwise occurred) was added followed by evaporation once again. This process was repeated three times to ensure removal of unreacted monomer. Some secondary nucleation occurred during polymerization (yielding a secondary distribution of particles with a number-average diameter (d_n) of approx. 300 nm as estimated by dynamic light scattering). To remove these particles, an aqueous solution of PVA was added to the concentrated emulsion obtained above, followed by centrifugation at 2000 rpm and subsequent removal of the upper layer (containing the particles from secondary nucleation) by decantation (this process was repeated three times). The particles were subsequently washed with water (followed by centrifugation and decantation, repeated three times) to remove PVA. After decantation, methanol was added, and the particles were isolated by filtration using a PTFE filter of pore size 0.2 μm, and subsequent drying under vacuum at room temperature. The polymer particles prepared by NMP were isolated according to a similar procedure, except there was no need to remove particles from secondary nucleation (no secondary nucleation occurred).

2.3. Measurements

S and DVB conversions were determined by gas chromatography (Shimadzu Corporation, GC-2014) with helium as the carrier gas, and employing tetrahydrofuran (THF) as solvent and *p*-xylene as internal standard. MWDs were measured by gel permeation chromatography (GPC) with two S/DVB gel columns (TOSOH Corporation, TSK gel GMH_{HR}-H, 7.8 mm i.d × 30cm) using THF as eluent at 40°C at flow rate of 1.0 mL · min^{-1} employing refractive index (TOSOH RI-8020/21) and ultraviolet detectors (TOYO SODA UV-8II). The columns were calibrated with six standard PS samples (1.05×10^3 - 5.48×10^6, M_w/ M_n = 1.01-1.15). All GPC samples were completely soluble in THF. The polymer particles were observed with a Hitachi S-2500 scanning electron microscope (SEM).

2.4. Compression tests

The mechanical properties of the polymer particles in the dry state were measured at room temperature by use of a micro compression testing machine (SHIMADZU DUH-W201) with a 50 μm diameter flat indenter at a rate of 0.14 mN/s. The micro-compression device was equipped with an optical microscope, thus enabling approximate estimation of the diameter of the single particle being tested, and thus also enabling one to select particles of suitable size within the distribution for testing. The particles tested were all in the approximate diameter range of 9 μm ± 1 μm. The compressive strength (σ_B) is related to the breaking load (P) and the particle diameter (d) according to Eq. (1) [32-35].

$$\sigma_B = a\frac{P}{d^2} \quad (1)$$

where "a" is a constant, the value of which depends on the relationship between the compressive and tensile stress in the center of the particle [33,34,36]. Eq. (1) was derived for a pair of concentrated loads (sharply pointed forces) being applied to a particle [34]. In the present study, the deformation at break was less than 10% in all cases, and thus the contact area between the particle and the indenter would not change too significantly on compression. The value of "a" is not known for the particles of the present study, and hence only the relative values of σ_B were calculated ($\sigma_{B,\,rel}$), using a sample of PS (no cross-linking) as reference point. Each data point reported (Fig. 8) corresponds to the average of twenty independent measurements.

3. Results and discussion

3.1. Rate of polymerization

Total conversion vs. time plots for S/DVB micro-suspension conventional radical polymerization (70°C) and NMP (125°C) show that both polymerizations proceeded smoothly to high conversion (Fig. 1). The rate of polymerization (R_p) in the NMP system is similar to the corresponding bulk system [37] (R_p in conventional radical copolymerization of S/DVB in bulk at low conversion is not affected by a DVB content as low as 1 mol% [38]). Recent modeling and simulations based on modified Smith-Ewart equations have indicated that compartmentalization effects for the S/TEMPO system at 125°C are not significant for particle diameters greater than approx. > 110 nm [39,40]. It has also been shown theoretically that partitioning of TEMPO to the aqueous phase has only negligible effects on R_p in the S/TEMPO system at 125°C [41].

The number of potential cross-links is governed by the apparent reactivity of DVB, i.e. the mol% of DVB units in the copolymer. Due to the low molar fraction of DVB, the monomer consumption by DVB-terminated radicals is negligible, and thus Eq. (2) applies [9]:

$$\ln\frac{[\mathrm{DVB}]_0}{[\mathrm{DVB}]} = \frac{k_{\mathrm{SDVB}}}{k_{\mathrm{SS}}}\ln\frac{[\mathrm{S}]_0}{[\mathrm{S}]} \qquad (2)$$

where k_{SS} denotes the propagation rate coefficient for S, k_{SDVB} is the rate coefficient for addition of a PS radical to DVB, and $[DVB]_0$ and $[S]_0$ denote initial concentrations. Fig. 2 shows a plot according to Eq. (2), where the straight lines are best fits of the respective data sets resulting in $k_{SS}/k_{SDVB} = r_S = 0.45$ in the conventional system and 0.38 in the NMP system, which lie within the range of values reported in the literature [42]. The relative consumption rates were equal in the two systems, and thus any differences in mechanical properties between the systems do not have their origin in the mol% of DVB in the copolymer. We previously reported that the rate of DVB consumption (relative to S) for the S/DVB/TEMPO/125 °C system in aqueous miniemulsion was lower than in bulk for sufficiently small particles [29,30].

3.2. Molecular weight distributions

Fig. 3 shows MWDs obtained at different conversions for the conventional system and the NMP system. Insoluble gel began to form in the conversion ranges 7 - 16% and 47 - 72% in the conventional system and the NMP system, respectively. The delayed gelation in the CLRP system is consistent with previous work on CLRP cross-linking radical polymerization in bulk/solution [9-14,21].

In the conventional system (Fig. 3a), the primary chain-length can be equated to the

number-average degree of polymerization (P_n) in the absence of cross-linking according to steady-state kinetics in a homogeneous system (exit/entry is not significant due to the large particle size and the use of an oil-phase initiator):

$$P_n = \frac{R_p}{R_i} = \frac{k_p[P\bullet][M]}{2fk_d[I]} = \frac{k_p[M]}{2fk_d[I]}\left(\frac{fk_d[I]}{k_t}\right)^{0.5} = k_p[M]\left(4fk_d[I]k_t\right)^{-0.5} \quad (3)$$

where k_p, k_t and k_d are the are the coefficients for propagation (assumed to be that of S; 480 $M^{-1}s^{-1}$ [43]), termination (1.17 x 10^8 $M^{-1}s^{-1}$ [44]) and BPO decomposition (1.19 x 10^{-5} s^{-1} [45]), respectively, f is the initiator efficiency (0.7), and M, I and P• denote monomer, initiator, and propagating radical, respectively, resulting in P_n = 583, i.e. M_n(primary chains) ≈ 61,000. The low MW peak in Fig. 3(a) therefore corresponds to primary chains. The much more prominent high MW shoulder in the conventional system than the NMP system at low conversion thus suggests that the number of intermolecularly (as opposed to intramolecularly) reacted pendants per chain was higher in the conventional system.

In the NMP system (Fig. 3b), the MWDs shifted to higher MW with increasing conversion, and a high MW shoulder appeared as a result of branching/cross-linking. The M_n values of the primary chains were estimated from the low MW peak (i.e. the total MWD minus the high MW shoulder) [17,18] by first determining M_n of the full MWD at 10% conversion. It was subsequently assumed that at this low conversion, the effect of branching/cross-linking on the MWD was negligible (as evidenced by the shape of the MWD and M_w/M_n = 1.30). The MWD of the primary chain-lengths was assumed to be independent of conversion (i.e. only shifting to higher MW with conversion), and thus the M_n values of the primary chains at higher conversions could be estimated according to the ratio between the y-value of the $w(\log M)$ vs. $\log M$ plot at the peak top and at M_n at 10% conversion. The resulting M_n values increased approximately linearly with conversion, close to the theoretical values ($M_{n,th}$) (Fig. 4; $M_{n,th}$ was calculated by treating DVB as S, i.e. according to $M_{n,th} = (\alpha[M]_0 M_M)/[TEMPO]_0$, where α is the total monomer conversion, $[M]_0$ denotes the total monomer concentration, and M_M was approximated as the MW of S. $M_{n,th}$ thus corresponds to M_n if the system proceeds according to the ideal CLRP mechanism in the absence of cross-linking. It can therefore be concluded that the polymerization proceeded in a living manner.

3.3. Compressive strength

Fig. 5 and 6 shows SEM photographs of P(S/DVB) particles prepared by conventional radical polymerization (after centrifugal washing (Fig. 5)) and NMP (Fig. 6). Significant secondary nucleation (d_n ≈ 300 nm) was evident in the conventional system, but secondary nucleation was not

observed in the NMP system. Secondary nucleation has previously been observed in similar conventional (i.e. not CLRP) suspension polymerizations both in the presence and absence of a cross-linker. The addition of an aqueous phase radical scavenger substantially reduces or eliminates secondary nucleation both in the presence and absence of a cross-linker [46-48]. The partition coefficient of TEMPO between S and water ($[TEMPO\bullet]_S/[TEMPO\bullet]_{aq}$) at 135°C is 98.8 [49], i.e. the aqueous phase concentration of TEMPO in the present study is expected to be approx. 2.2×10^{-4} M, and this may have prevented secondary nucleation from occurring in the NMP system. The particles obtained in the conventional system were thoroughly washed prior to mechanical testing to ensure removal of all smaller particles generated by secondary nucleation (the MWDs in Fig. 3(a) correspond to the washed particles).

The micro compression testing machine enables measurement of individual particles (as opposed to a cluster of particles), and the results thus truly represent the mechanical properties of a single particle as opposed to the bulk properties of the material. Similar experimental approaches to measure mechanical properties of polymer particles have been reported for cross-linked poly(ethylene glycol) particles [50] and poly(acrylic acid) particles [51], as well as for stainless steel particles [52]. The primary data obtained by the compression tests are load (mN) vs. deformation (μm) as shown in Fig. 7 for a representative sample (NMP system at 93% conversion). The breaking load (*P*) and the deformation at break were defined based on the point at the beginning of the plateau region as indicated in Fig. 7. The two optical micrographs in Fig. 7 show the particle viewed from above (along the axis of loading) at points (a) and (b). The dark wedge-shaped sections near the edge of the particle are cracks (Fig. 7b). In this way, it was confirmed experimentally by visual observation that all particles tested did indeed break similarly to the specific example given in Fig. 7. The relative compressive strength ($\sigma_{B,\,rel}$) was subsequently calculated from Eq. (1), using the PS particle (no cross-linking) as a reference point ($\sigma_{B,\,rel} = \sigma_{B,\,sample}/\sigma_{B,\,PS}$).

Values of $\sigma_{B,\,rel}$ were obtained as a function of conversion for the conventional and the NMP systems (Fig. 8). The polymer particles were monomer-free even at low conversion, because unreacted monomer was removed prior to mechanical testing (see Experimental section). The values of $\sigma_{B,\,rel}$ for the conventional system remained close to constant throughout the entire conversion range investigated (7-96%), whereas an approximately linear increase in $\sigma_{B,\,rel}$ with conversion was observed in the NMP system. At low/intermediate conversion (< approx. 50%), the $\sigma_{B,\,rel}$ values of the conventional system were markedly higher than for the NMP system, whereas similar results were obtained at high conversion (> approx. 70%).

Network formation in a CLRP system differs significantly from that in a conventional system

[9,10,21]. In a conventional cross-linking system, the high MW of the primary chains and the resulting relatively high concentration of pendant unsaturations in the vicinity of the radical chain end results in significant intramolecular cross-linking and formation of microgels at relatively low conversion, and these microgels are subsequently linked by further reactions of pendant unsaturations to yield a very non-homogeneous network. In a CLRP system, the MW of the primary chains is much lower than in a conventional system, and the local concentration effect of unsaturated pendants around the radical center (as in a conventional system) is essentially absent. As such, the relative amount of intermolecular cross-linking is expected to be higher than in the corresponding conventional system, microgel formation does not occur (or is much less prominent) and a more homogeneous network is formed.

The results in Fig. 8 can thus be rationalized qualitatively as follows: In the conventional system, there was essentially no change in $\sigma_{B,\,rel}$ with conversion, suggesting that microgels (formed already at low conversion) made a significant contribution towards $\sigma_{B,\,rel}$. In the NMP system, $\sigma_{B,\,rel}$ increased with conversion due to a continuous increase in the number of intermolecular cross-links per primary chain (in a CLRP system, the primary chain-length increases linearly with conversion, whereas it remains close to constant in a conventional system prior to the gel-effect). The value of $\sigma_{B,\,rel}$ (according to our definition, $\sigma_{B,\,rel} = 1$ for PS with no cross-linking) in the absence of cross-linking (S homopolymer; Fig. 8) at high conversion (93%) was as anticipated somewhat lower than for both cross-linking systems at similar conversions, but significantly higher than $\sigma_{B,\,rel}$ of the NMP cross-linking system at low/intermediate conversion (≤ 47%). The narrow MWD of the NMP system at 10% (M_w/M_n = 1.30) indicates that the vast majority of chains had not undergone cross-linking (gelation occurred in the conversion range 47 - 72%). The value of $\sigma_{B,\,rel}$ was thus higher than for the NMP P(S-DVB) particles at low/intermediate conversion (≤ 47%) due to the much higher MW in the linear PS particles (M_n = 76,000, M_w/M_n = 2.33).

The deformation at break and the breaking energy are displayed vs. conversion in Fig. 9(a) and (b), respectively. Both plots exhibit trends similar to the compressive strength vs. conversion plots (Fig. 8). The deformation at break and the breaking energy remained approximately constant with conversion for the conventional system (although there is considerable scatter), but increased close to linearly with conversion for the NMP system. These results are also consistent with the anticipated differences in network development between the two systems.

4. Conclusions

The mechanical properties of individual (not clusters of particles) micron-sized, cross-linked

P(S-DVB) particles (1 mol% DVB) prepared by conventional radical copolymerization (70°C) and nitroxide (TEMPO)-mediated radical copolymerization (125°C) in aqueous micro-suspension have been investigated. In the conventional system, the compressive strength, the deformation at break, and the breaking energy remained approx. constant from low to high conversion. However, all three quantities increased close to linearly with conversion in the case of NMP. The observed differences at low/intermediate conversion (< approx. 50%) have their origin in the different network formation mechanisms in the conventional and the NMP system. The main factor is believed to be microgel formation, which occurs already at low conversion in the conventional system, but is largely absent in the NMP system. At high conversion (> approx. 70%), the compressive strength, the deformation at break and the breaking energy of the particles were very similar in the two systems. The results indicate that network formation is more homogeneous in the NMP system than the conventional system.

Acknowledgements

This work was partially supported by the Support Program for Start-ups from Universities (No. 1509) from the Japan Science and Technology Agency (JST), a Grant-in-Aid for Scientific Research (Grant 17750109) from the Japan Society for the Promotion of Science (JSPS), and a Kobe University Takuetsu-shita Research Project Grant.

References

[1] Okubo M, Nakagawa T. Colloid Polym. Sci. 1992;270:853.

[2] Okubo M, Katayama Y, Yamamoto Y. Colloid Polym. Sci. 1991;269:217.

[3] Song J-S, Winnik MA. Macromolecules 2005;38:8300.

[4] Thomson B, Rudin A, Lajoie G. J. Appl. Polym. Sci. 1996;59:2009.

[5] Okubo M, Minami H, Komura T. J. Appl. Polym. Sci. 2003;88:428.

[6] Okubo M, Minami H, Jing Y. J. Appl. Polym. Sci. 2003;89:706.

[7] Okubo M, Konishi Y, Minami H. Colloid Polym. Sci. 2003;124:54.

[8] Matyjaszewski K Advances in controlled/living radical polymerization. Washington, DC: American Chemical Society, 2003.

[9] Ide N, Fukuda T. Macromolecules 1997;30:4268.

[10] Ide N, Fukuda T. Macromolecules 1999;32:95.

[11] Yu Q, Zeng F, Zhu S. Macromolecules 2001;34:1612.
[12] Jiang C, Shen Y, Zhu S, Hunkeler D. J. Polym. Sci., Part A: Polym. Chem 2001;39:3780.
[13] Nagelsdiek R, Mennicken M, Maier B, Keul H, Hocker H. Macromolecules 2004;37:8923.
[14] Wang AR, Zhu S. Polym. Eng. Sci. 2005;45:720.
[15] Anandkumar AR, Anderson KJ, Anseth JW, Bowman CN. J. Polym. Sci., Part B: Polym. Phys. 1997;35:2297.
[16] Anandkumar AR, Anseth JW, Bowman CN. Polymer 1998;39:2507.
[17] Wang AR, Zhu S. J. Polym. Sci.; Part A: Polym. Chem. 2005;43:5710.
[18] Li Y, Armes SP. Macromolecules 2005;38:8155.
[19] Georges MK, Veregin RPN, Kazmaier PM, Hamer GK. Macromolecules 1993;26:2987.
[20] Goto A, Fukuda T. Prog. Polym. Sci. 2004;29:329.
[21] Norisuye T, Morinaga T, Tran-Cong-Miyata Q, Goto A, Fukuda T, Shibayama M. Polymer 2005;46:1982.
[22] Qiu J, Charleux B, Matyjaszewski K. Prog. Polym. Sci. 2001;26:2083.
[23] Cunningham MF. Prog. Polym. Sci. 2002;27:1039.
[24] Okubo M, Minami H, Zhou J. Colloid Polym. Sci. 2004;282:747.
[25] Kagawa Y, Minami H, Okubo M, Zhou J. Polymer 2005;46:1045.
[26] Prescott SW, Ballard MJ, Rizzardo E, Gilbert RG. Aust. J. Chem. 2002;55:415.
[27] Nicolas J, Charleux B, Guerret O, Magnet S. Macromolecules 2004;37:4453.
[28] Li M, Matyjaszewski K. J. Polym. Sci., Part A: Polym. Chem 2003;41:3606.
[29] Zetterlund PB, Alam MN, Minami H, Okubo M. Macromol. Rapid Commun. 2005;26:955.
[30] Alam MN, Zetterlund PB, Okubo M. Macromol. Chem. Phys. 2006;207:1732.
[31] Nakajima Y, Shimizu M. J. Mineralogical Soc. Jpn. 1988;18:393.
[32] Hiramatsu Y, Oka Y, Kiyama H. Nihonkougyoukaishi 1965;81:1024.
[33] Munkholm LJ, Kay BD. Soil Sci. Soc. Am. J. 2002;66:702.
[34] Hiramatsu Y, Oka Y. Int. J. Rock Mech. Min. Sci. 1966;3:89.
[35] Imhoff S, Silva APd, Dexter A. Soil Sci. Soc. Am. J. 2002;66:1656.
[36] Dexter AR. J. Terramechanics 1975;12:3.
[37] Fukuda T, Terauchi T, Goto A, Ohno K, Tsujii Y, Miyamoto T, Kobatake S, Yamada B. Macromolecules 1996;29:6393.
[38] Zetterlund PB, Yamazoe H, Yamada B. Polymer 2002;43:7027.
[39] Zetterlund PB, Okubo M. Macromolecules 2006;39:8959.
[40] Zetterlund PB, Okubo M. Macromol. Rapid Commun. 2007;16:221.
[41] Zetterlund PB, Okubo M. Macromol. Theory Simul. 2005;14:415.
[42] Greenley RZ. Free radical copolymerization reactivity ratios. In: Brandrup, J, Immergut, EH,

Grulke, EA, editors. Polymer handbook. 4th ed. New York: John Wiley & Sons; 1999. pp. II/254

[43] Buback M, Gilbert RG, Hutchinson RA, Klumperman B, Kuchta FD, Manders BG, O`Driscoll KF, Russell GT, Schweer J. Macromol. Chem. Phys. 1995;196:3267.

[44] Buback M, Kowollik C, Kurz C, Wahl A. Macromol. Chem. Phys. 2000;201:464.

[45] Dixon KW. Decomposition rates of Organic Free Radical Initiators. In: Brandrup, J, Immergut, EH, Grulke, EA, editors. Polymer handbook. 4th ed. New York: John Wiley & Sons; 1999. pp. II/12

[46] Yuyama H, Hashimoto T, Ma G-H, Nagai M, Omi S. J. Appl. Polym. Sci. 2000;78:1025.

[47] Ma G-H, Nagai M, Omi S. J. Appl. Polym. Sci. 2001;79:2408.

[48] Ma G-H, Chen A-Y, Su Z-G, Omi S. J. Appl. Polym. Sci. 2003;87:244.

[49] Ma JW, Cunningham MF, McAuley KB, Keoshkerian B, Georges MK. J. Polym. Sci., Part A: Polym. Chem 2001;39:1081.

[50] Egholm RD, Christensen SF, Szabo P. J. Appl. Polym. Sci. 2006;102:3037.

[51] Knaebel A, Rebre SR, Lequeux F. Polymer Gels and Networks 1997;5:107.

[52] Hashimoto H, Sun ZM, Abe T. Scripta Materialia 2003;49:997.

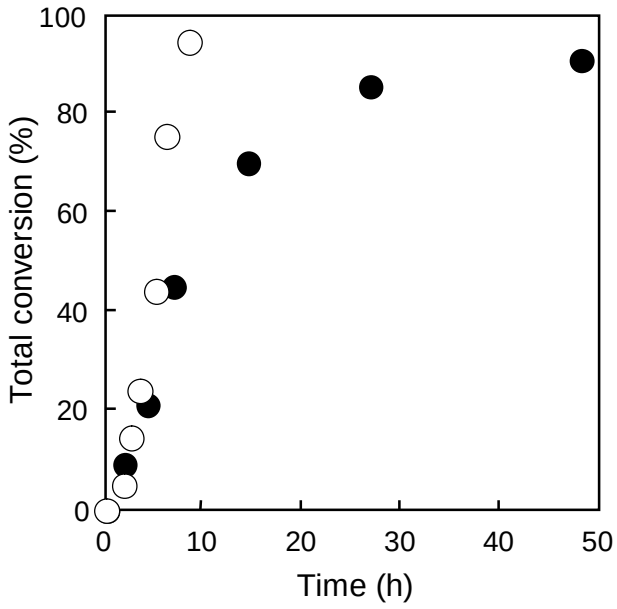

Figure 1. Total conversion vs. time plots for aqueous micro-suspension copolymerizations of S (99 mol%) and DVB (1 mol%): Conventional radical polymerization (○) at 70˚C with $[BPO]_0 = 1.3 \times 10^{-2}$ M; NMP (●) at 125˚C with $[BPO]_0 = 1.3 \times 10^{-2}$ M and $[TEMPO]_0 = 2.2 \times 10^{-2}$ M

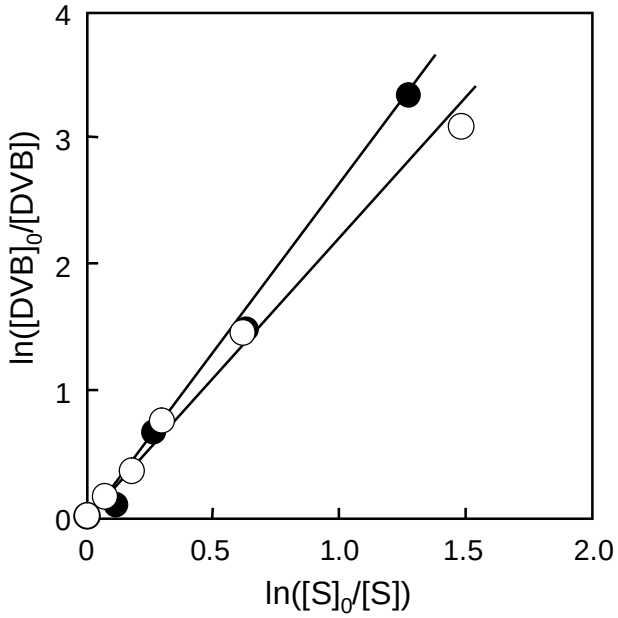

Figure 2. ln([DVB]$_0$/[DVB]) vs. ln([S]$_0$/[S]) plots for aqueous micro-suspension copolymerizations of S (99 mol%) and DVB (1 mol%): Conventional radical polymerization (○) at 70˚C with [BPO]$_0$ = 1.3 × 10^{-2} M; NMP (●) at 125˚C with [BPO]$_0$ = 1.3 × 10^{-2} M and [TEMPO]$_0$ = 2.2 × 10^{-2} M. The lines are best fit of the terminal model.

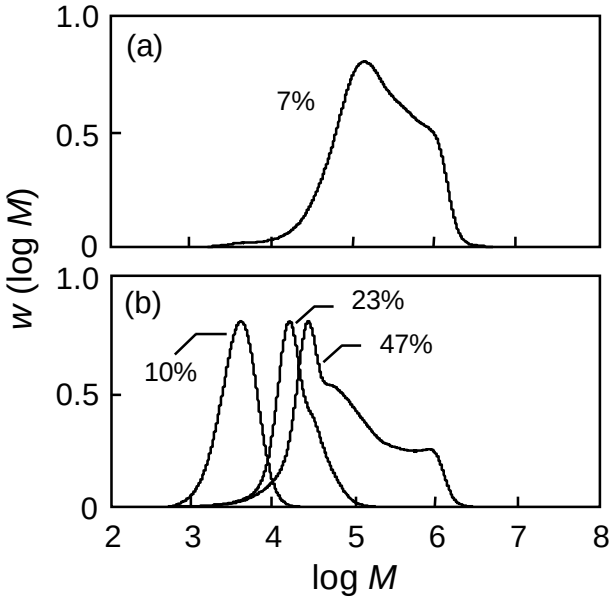

Figure 3. Molecular weight distributions of primary chains for the aqueous micro-suspension copolymerizations of S (99 mol%) and DVB (1 mol%): (a) Conventional radical polymerization at 70˚C with $[BPO]_0 = 1.3 \times 10^{-2}$ M; (b) NMP at 125˚C with $[BPO]_0 = 1.3 \times 10^{-2}$ M and $[TEMPO]_0 = 2.2 \times 10^{-2}$ M. Conversions as indicated.

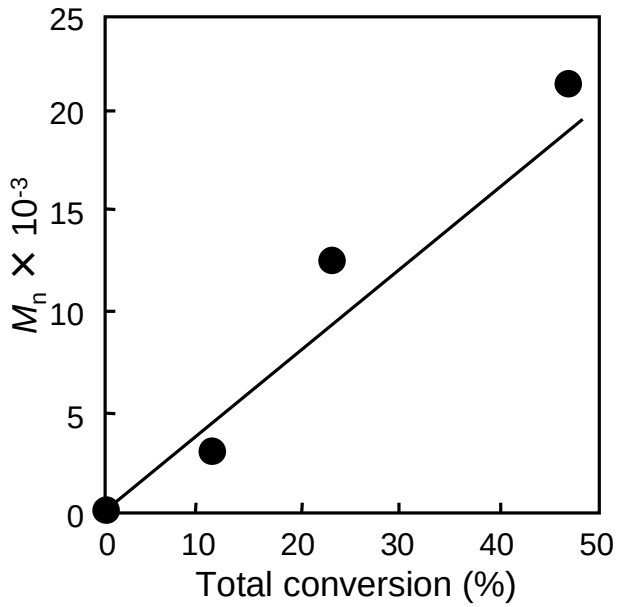

Figure 4. Number-average molecular weights (M_n) of primary chains in the aqueous micro-suspension NMP of S (99 mol%) and DVB (1 mol%) at 125°C with $[BPO]_0 = 1.3 \times 10^{-2}$ M and $[TEMPO]_0 = 2.2 \times 10^{-2}$ M. The line is the theoretical M_n ($M_{n,th}$) based on no cross-linking.

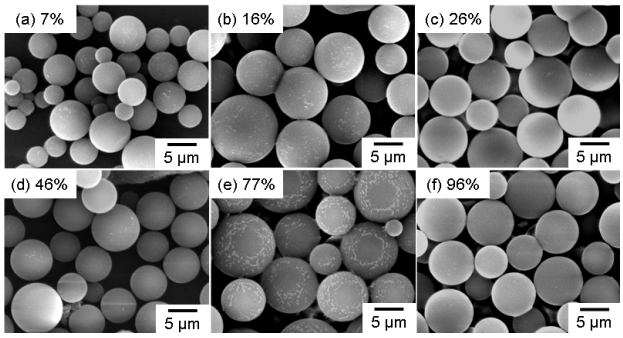

Figure 5. SEM photographs of P(S-DVB) particles prepared by aqueous micro-suspension conventional radical polymerization of S (99 mol%) and DVB (1 mol%) at 70°C, after centrifugal washing. Conversions as indicated.

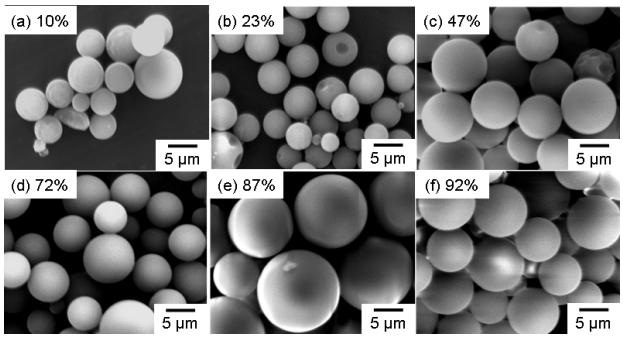

Figure 6. SEM photographs of P(S-DVB) particles prepared by aqueous micro-suspension NMP of S (99 mol%) and DVB (1 mol%) at 125°C. Conversions as indicated.

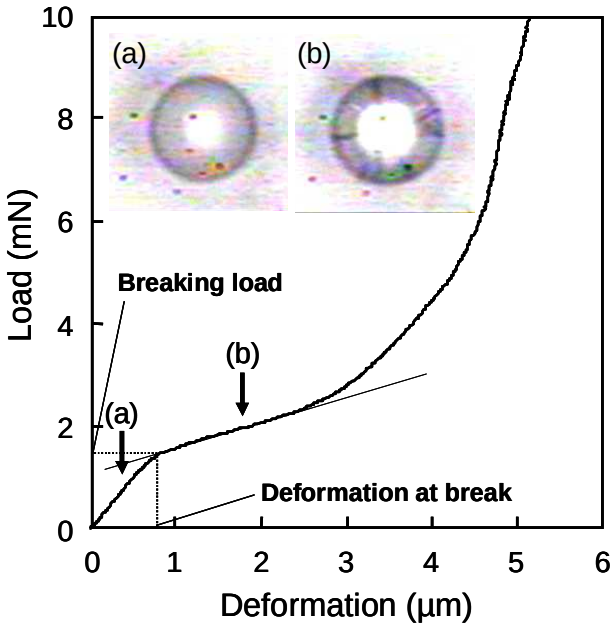

Figure. 7 Load vs. deformation measured by micro compression testing machine at a rate of 0.14 mN/s for P(S-DVB) particles (NMP system at 93% conversion). The photos show the particle viewed from above (along the axis of loading) at the points (a) and (b).

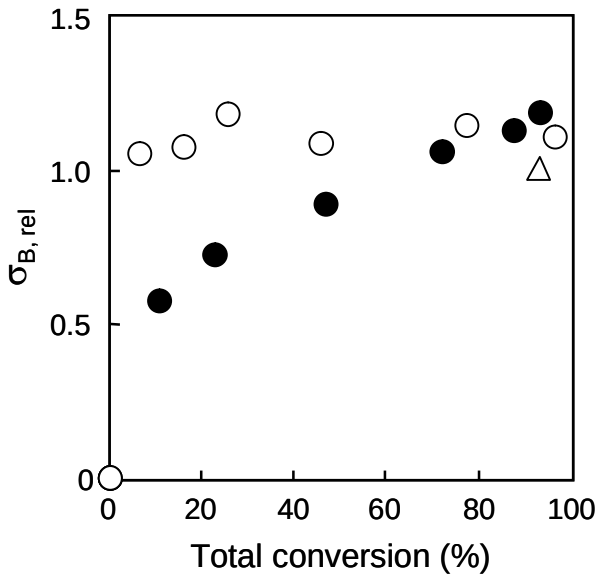

Figure 8. Relative compressive strength ($\sigma_{B,\,rel}$; normalized to PS sample without cross-linking (△)) vs. total conversion for P(S-DVB) particles prepared by conventional radical polymerization (○) and NMP (●) in aqueous micro-suspension.

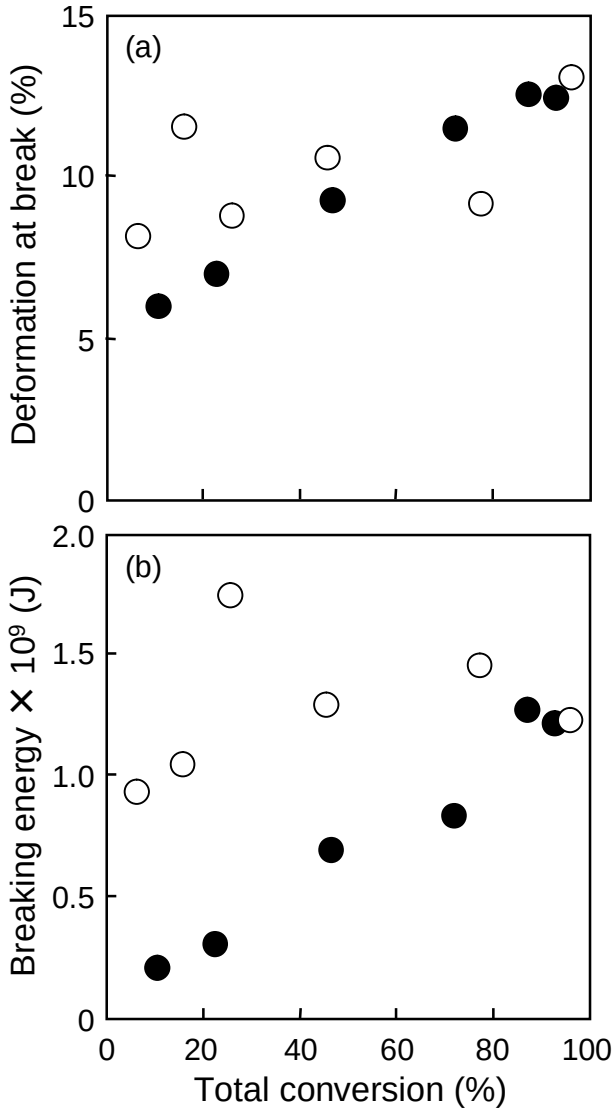

Figure 9. (a) Deformation at break vs. total conversion and (b) breaking energy vs. total conversion for P(S-DVB) particles prepared by conventional radical polymerization (○) and NMP (●) in aqueous micro-suspension.